Silicone Oil-Water Interaction and Emulsification Visual Simulation for Intraocular Silicone Oil Tamponade

1st Chongming Song
School of Computer and Communication Engineering, University of Science and Technology Beijing
Beijing, China
18519225284@163.com

2nd Yanrui Xu
Institute of Artificial Intelligence, University of Science and Technology Beijing
Beijing, China
xuyanruiedw@me.com

3rd Xiaokun Wang*
Beijing Advanced Innovation Center for Materials Genome Engineering, University of Science and Technology Beijing
Beijing, China
wangxiaokun@ustb.edu.cn

4th Jiamin Wang
School of Computer and Communication Engineering, University of Science and Technology Beijing
Beijing, China
no4724722205@163.com

5th Houbin Huang
Department of Ophthalmology, Chinese PLA General Hospital
Beijing, China
huanghoubin@hotmail.com

6th Zhihong Zhu
Department of Ophthalmology, Hainan Hospital of PLA General Hospital
Hainan, China
zhuzhi258@163.com

7th Xiaojuan Ban*
Beijing Key Laboratory of Knowledge Engineering for Materials Science, University of Science and Technology Beijing
Beijing, China
banxj@ustb.edu.cn

***Abstract*—Vitrectomy combined with silicone oil tamponade is an effective treatment for rhegmatogenous retinal detachment (RRD). The high viscosity and surface tension of the silicone oil make it suitable for treating large retinal tears by pressing against the retina. However, silicone oil becomes emulsified over time as it remains in the eye, which can cause serious complications. Clear visual acquisitions of silicone oil-water interaction and silicone oil emulsification progress are difficult during and after the surgery. To help doctors and patients perceive the two-phase interaction and emulsification progress intuitively, we propose a physically based simulation method for intraocular silicone oil visualization. For the visualization of immiscible silicone oil-water interaction, we introduce a volume-incompressible Smoothed Particle Hydrodynamics (SPH) approach to improve simulation precision of multiphase flow coupling. A diffusion model based on volume fraction is proposed to visualize emulsification progress. Additionally, we combine our method with cohesion and surface-minimization driven surface tension model to describe the high surface tension of silicone oil. Experiments show that our scheme can obtain a precise pressure gradient near phase boundary and perform noticeable mixing effect that evolves over time. Our method has the advantage of higher accuracy than other visualization methods, and has the potential to help doctors make decisions and estimate surgical outcomes.**

***Index Terms*—Medical visualization; Rhegmatogenous retinal detachment; Silicone oil tamponade; Multiphase flows simulation**

*Corresponding authors.

I. Introduction

Rhegmatogenous retinal detachment (RRD) is characterized by retinal tears with fluid accumulating between separated retinal neurosensory layer and retinal pigment epithelium layer. Pars Plana Vitrectomy (PPV) combined with silicone oil tamponade has become one of the major treatments as the primary repair for RRD, as shown in Figure 1.

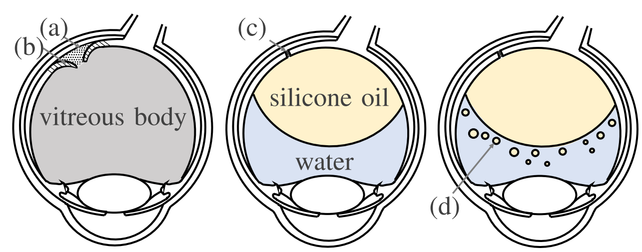

Fig. 1. Procedure of PPV combined with silicone oil tamponade. Left: original condition of rhegmatogenous retinal detachment: liquid (a) accumulates behind the retina tear (b). Middle: silicone oil tamponade with vitreous body being removed after reattaching the retina (c). Right: silicone oil emulsification (d) over time.

Silicone oil is a popular kind of intraocular filler [1] for RRD for its relative safety and preferable optical and mechanical properties. However, silicone oil becomes emulsified in the vitreous chamber over time, impairing the operation's effectiveness and causing various complications such

2021 IEEE International Conference on Bioinformatics and Biomedicine (BIBM) | 978-1-6654-0126-5/21/$31.00 ©2021 IEEE | DOI: 10.1109/BIBM52615.2021.9669305

as proliferative vitreoretinopathy, recurrent retinal detachment, intraocular inflammation and secondary glaucoma.

As the emulsification process within the vitreous chamber is difficult to fully observe in reality, developing a computer simulation method to visualize silicone oil condition can help to better understand the process. Potential uses of such a visualization system include making demonstrations to patients or students, and simulating real surgeries to assist doctors to make decisions about quantifying silicone oil needed to be filled and the time to remove it.

Currently, there is a lack of simulation and visualization methods for silicone oil emulsification. We propose a physics-based visual simulation method for the silicone oil-water two phase interaction and emulsification after silicone oil tamponade. In summary, the main contributions of our method are:

- a two-way coupling framework for volume-incompressible fluids that is capable of handling various density ratios between silicone oil and water;
- a surface tension model that incorporates the effects of cohesion and curvature forces to minimize surface area;
- a multiphase mixture model based on volume fraction scheme for the simulation of mixing states between silicone oil and water.

II. Related Work

A. Silicone Oil Tamponade and Emulsification

In 1929, Gonin first realized that sealing the retinal tear is the key to the treatment of retinal detachment. In 1962, Cibis et al. [2] first applied silicone oil as a vitreous substitute in retinal detachment surgery. In the 1970s, Machemer [1] invented closed vitrectomy, which removes the vitreous body and then injects filler such as silicone oil, in order to recover the eye volume, separate the retina from adhering membranes, and smooth the detached retina.

Silicone oil emulsification refers to a process where silicone oil droplets separate from the main silicone oil bubble and diffuse into the eye tissue [3]. Silicone oil emulsification can cause several complications. If the silicone oil droplets enter the anterior chamber, they will affect the metabolism of aqueous humor, and adhere to the corneal endothelium, causing corneal decompensation, and other corneal diseases [4] [5]. Emulsified silicone oil can also cause proliferative vitreoretinopathy, recurrent retinal detachment, intraocular inflammation, secondary glaucoma and other diseases [6]. In addition, long-term retention of silicone oil in the eye can induce complicated cataracts, reduce choroidal thickness, and cause retinal degeneration [7].

B. Physics-based Fluid Simulation

Physics-based fluid simulation uses physical rules to simulate fluids visually and realistically, which can model the interactive behaviour of water and silicone oil within the eye.

The Smoothed Particle Hydrodynamics (SPH) approach is a physics-based fluid simulation method using particle-based fluid representation and numerical time integration [8], which is good at capturing fluid details. Becker et al. [9] proposed Tait equation-based Weakly Compressible SPH (WCSPH) method. Subsequently, implicit iterative SPH solvers [10] [11] were proposed to enforce the incompressibility of the fluid. The state-of-the-art SPH solver, Divergence-Free SPH (DFSPH) [12], contains two iterative solvers: a divergence free solver and a constant density solver.

For multiphase simulation involving interactions and mixing between two or more kinds of liquid (e.g. silicone oil and water), Müller et al. [13] introduced the diffusion equation. The concept of volume fraction [14] and corresponding mixing models [15] were introduced to better capture miscibility and were integrated into an iterative SPH solver [16]. Helmholtz free energy [17] has been used to improve the mixing behavior; and conservative phase field equations [18] were used to achieve higher Reynolds number and density ratios.

III. Physics-based Simulation of Silicone Oil Emulsification and Diffusion

To simulate the multiphase fluid interaction between silicone oil and water during silicone oil tamponade process, the motion of fluids, the surface tension effect, and diffusion due to emulsification all need to be considered.

We first introduce a volume-incompressible SPH method that derives pressure fields according to volume incompressibility instead of density, which avoids the numerical error that results from non-uniform density fields of the multiphase flow. Secondly, we model cohesion and curvature force to simulate the effect of surface tension between the two phases. Thirdly, we introduce a volume fraction-based multiphase mixture model to simulate the diffusion between water and emulsified silicone oil. The simulation procedure is listed in Algorithm 1.

A. Pressure Model for Incompressible Multiphase Fluid

1) SPH Fluid Simulation: The SPH method discretizes continuous medium into computable macro particles [19]. It approximates any continuous field value $A(\boldsymbol{x}_i)$ (abbreviated A_i) at the position $\boldsymbol{x}_i$ of a given particle i, from the values A_j of all neighboring particles j within the support radius h, shown in Figure 2, as:

$$A_i = \sum_j A_j \frac{m_j}{\rho_j} W(\boldsymbol{x}_i - \boldsymbol{x}_j, h), \tag{1}$$

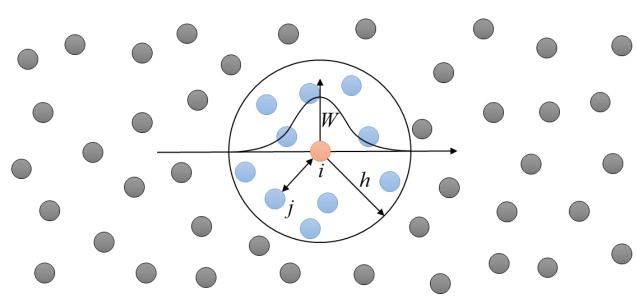

Fig. 2. Schematic diagram of the SPH approximation

In Eqn. (1), m_j and ρ_j represent mass and density of j; and $W(\boldsymbol{x}_i - \boldsymbol{x}_j, h)$ (shortened as W_{ij}) is a cubic spline function called the smoothing kernel [12].

However, in multiphase simulations where the particle mass is non-uniform, numerical error would occur when approximating the density ρ using the traditional Eqn. (1). Inspired by [20], we establish the volume-incompressible multiphase SPH method by substituting m_i/ρ_i with the particle's volume V_i, and reform the SPH discretization as:

$$A_i = \sum_j A_j V_j W_{ij}. \tag{2}$$

We then define a coressponding notion called "compression rate" Γ to represent the extent to which the particle is compressed:

$$\Gamma_i = \frac{V_i^0}{V_i} = \sum_j V_j^0 W_{ij}, \tag{3}$$

where V_i^0 is the rest volume, which is the particle's actual volume without any compression.

Since only W_{ij} is a non-constant function with respect to $\boldsymbol{x}_i$ in Eqn. 2, the gradient of A_i can be straightforwardly approximated as:

$$\nabla A_i = \sum_j A_j V_j \nabla W_{ij}. \tag{4}$$

As for the Laplacian operator, we apply the same approximate form as in [19].

In physics, the motion of incompressible fluid flow is governed by the Navier-Stocks equation, as:

$$\rho \frac{D\boldsymbol{v}}{Dt} = -\nabla p + \mu \nabla^2 \boldsymbol{v} + \rho \mathbf{g}, \tag{5}$$

where μ is the dynamic viscosity, p is the pressure, $\boldsymbol{v}$ is the fluid velocity, $\mathbf{g}$ is gravity acceleration, D/Dt presents the material derivative.

In terms of computing the pressure gradient ∇p, our method is similar to DFSPH [12]. We first assume that the pressure is proportional to volume change:

$$\nabla p_i = \nabla \left(\kappa_i \left(V_i^0 - V_i \right) \right) = \kappa_i V_i^0 \sum_j \frac{V_j^0}{\Gamma_j^2} \nabla W_{ij}, \tag{6}$$

where κ_i is an unknown rigidity coefficient. Then, we implicitly solve the pressure so that the pressure force makes every particle non-compressed.

B. Silicone Oil-water Surface Tension Modeling

To depict the strong surface tension of the silicone oil, we apply the cohesion force model and a curvature force that minimizes the surface area within each phase [21].

The curvature force aiming at minimizing surface area, from particle j to particle i, is:

$$\boldsymbol{F}_{i \leftarrow j}^{cur} = -\gamma m_i (\boldsymbol{n}_i - \boldsymbol{n}_j), \tag{7}$$

where $\boldsymbol{n}$ is the normal to the surface of the given phase, and γ is the surface tension coefficient denoting the magnitude of the surface tension. The normal to the surface can be calculated using the color field: $c_i = \sum_j V_j W_{ij}$. Fluid particles located on the surface, due to a lack of neighbors, have smaller color field values c than those with full neighbors. The surface normal can be obtained with the color field gradient using Eqn. (4):

$$\boldsymbol{n}_i = h \nabla c_i = h \sum_j V_j \nabla W_{ij}. \tag{8}$$

The second term, cohesion force, is expressed as the mutual attraction between the particles representing the same fluid phase. The attraction depending on the distance between particles is:

$$\boldsymbol{F}_{i \leftarrow j}^{coh} = -\gamma m_i m_j \frac{\boldsymbol{x}_i - \boldsymbol{x}_j}{|\boldsymbol{x}_i - \boldsymbol{x}_j|} C\left(|\boldsymbol{x}_i - \boldsymbol{x}_j|\right), \tag{9}$$

where $C(l)$ is a normalized spline function for cohesion force (refer to [21]).

Algorithm 1 Silicone oil emulsification and diffusion simulation solver

Input: Scenario initialization

set up global attributes: phase rest density ρ_k, dynamic viscosity μ, surface tension coefficient γ, convection term C_m and diffusion term D_m

initialize discretized particles' attributes: particle location at time t: $\boldsymbol{x}(t)$, velocity $\boldsymbol{v}(t)$, volume fraction $\alpha(t)$, and rest volume V^0

Volume-incompressible computation

- compute compression rate Γ — Eqn. (3)
- compute pressure force $-\nabla p$ — Eqn. (6)
- compute particle acceleration $D\boldsymbol{v}/Dt$ — Eqn. (5)

Surface tension modeling

- derive surface normal — Eqn. (8)
- compute curvature force $\boldsymbol{F}^{cur}$ — Eqn. (7)
- compute cohesion force $\boldsymbol{F}^{coh}$ — Eqn. (9)
- update particle acceleration $D\boldsymbol{v}/Dt + (\boldsymbol{F}^{cur} + \boldsymbol{F}^{coh})/m$
- update particle position $\boldsymbol{x}$

Multiphase mixture visualization

- compute interphase momentum term $\boldsymbol{F}_k$ — Eqn. (11)
- compute drift velocity $\boldsymbol{v}_k^d$ — Eqn. (12)
- update volume fraction α_k — Eqn. (13)
- update particle mass m

Output: Particle state of the next time step

update particles' attributes after simulation time step spanned Δt: location $\boldsymbol{x}(t+\Delta t)$, velocity $\boldsymbol{v}(t+\Delta t)$, volume fraction $\alpha(t+\Delta t)$, mass $m(t+\Delta t)$

C. Volume Fraction Mixture Model for Visualizing Silicone Oil Emulsification

1) Volume Fraction Scheme: For the emulsification and diffusion effect between silicone oil and water, we introduce a volume-fraction based diffusible multiphase mixture model. In this model, each particle can carry multiple phases, and each phase occupies a fraction α_k of the particle's volume, where k labels the phase, and satisfies $\sum_k \alpha_{k_i} = 1$, as shown in Figure

3. According to the Local Equilibrium Assumption (LEA) [22], all phases are thoroughly mixed within each particle.

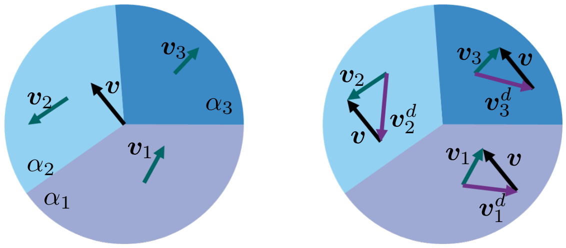

(a) (b)

Fig. 3. Particles with mixed phases. (a) Relationship between volume fraction α_k, phase velocity $\boldsymbol{v}_k$ and mixture velocity $\boldsymbol{v}$; (b) The relationship between $\boldsymbol{v}_k$, $\boldsymbol{v}$, and drift velocity $\boldsymbol{v}_k^d$.

The velocity at the volume center of each particle can be expressed with the mixture velocity: $\boldsymbol{v}_i = \sum_k \alpha_{k_i} \boldsymbol{v}_{k_i}$, where $\boldsymbol{v}_{k_i}$ is the phase velocity of phase k within particle i. The rest density of each particle satisfies $\rho_i^0 = \sum_k \alpha_{k_i} \rho_k$, where ρ_k is the rest density of each fluid phase. The drift velocity is $\boldsymbol{v}_{k_i}^d = \boldsymbol{v}_{k_i} - \boldsymbol{v}_i$, describing the relative velocity of each phase to the volume center of the particle.

2) Dynamic Model for Multiphase Flow: We incorporate the multiphase mixture model from [22]. In the multiphase model, each phase k in the particle i has an interface momentum source $\boldsymbol{F}_{k_i}$ that affect the phase velocity:

$$\begin{aligned} \alpha_{k_i} \rho_{k_i} \frac{D\boldsymbol{v}_{k_i}}{Dt} = \alpha_{k_i} (&-p_{k_i} + \mu_k \nabla^2 \boldsymbol{v}_i \\ &+ \rho_{k_i} \mathbf{g} - \rho_{k_i} \boldsymbol{v}_{k_i}^d \cdot \nabla) \boldsymbol{v}_{k_i} + \boldsymbol{F}_{k_i}, \end{aligned} \tag{10}$$

which satisfies $\sum_k \boldsymbol{F}_{k_i} = 0$ because of the conservation of momentum inside each particle.

By summing up Eqn. (10) for all phases, we can derive the relationship between the velocity of each particle and that of every single phase inside each of it according to [22]:

$$\boldsymbol{F}_{k_i} = \alpha_{k_i} (\rho_{k_i} - \rho_i) \left(\mathbf{g} - \frac{D\boldsymbol{v}_i}{Dt} \right). \tag{11}$$

From Eqn. (10) and Eqn. (11), the relationship between drift velocity and particle motion can be further established as:

$$\frac{D\boldsymbol{v}_{k_i}^d}{Dt} = \frac{\rho_{k_i} - \rho_i}{\rho_{k_i}} \left(\mathbf{g} - \frac{D\boldsymbol{v}_i}{Dt} \right). \tag{12}$$

3) Volume Fraction Update Mechanism: For each time step, the update of volume fraction involves a control factor and a diffusion item:

$$\alpha_{k_i} := \alpha_{k_i} \Delta t \left(-C_m \nabla \cdot (\alpha_{k_i} \boldsymbol{v}_{k_i}^d) + \nabla^2 (D_m \alpha_{k_i}) \right), \tag{13}$$

where C_m and D_m are parameters that respectively control inertial drag and diffusion.

IV. Experiments

In order to verify the effectiveness of our method, we first conduct an immiscible two-phase dambreak experiment to show the two-phase coupling effect. Next, we demonstrate miscibility with a miscible ink drop scene. Finally, we perform a realistic simulation of silicone oil tamponade and emulsification on an eye model.

The experiments are run on a computer with 16 GB RAM, an 8-core Intel® i7-9700 CPU at 3.00 GHz, and an Nvidia RTX 2080 SUPER GPU with 8.0 GB VRAM. The 2D simulation framework is written with the Taichi [23] language and runs on CUDA. For the 3D eye model experiment, we write a CPU-based simulation algorithm with C++ and OpenMP, using Eigen as mathematical library. We use the surface reconstruction method introduced in [24] to generate 3D meshes from particles, and Blender for offline rendering. Table I summarizes the experiments, which shows the number of particles used in each experiment, and displays the time cost of the experiments.

TABLE I
Experiment information.

Scene	Figure(s)	Particles	Time*
Two-phase coupling	Figs. 4, 5	116K	2.1
Ink drop	Figure 6	237K	55.9
Silicone oil tamponade	Figure 7	90K	35.4
Silicone oil emulsification	Figure 8	89K	168.9

*average time to run one second of simulation (minutes)

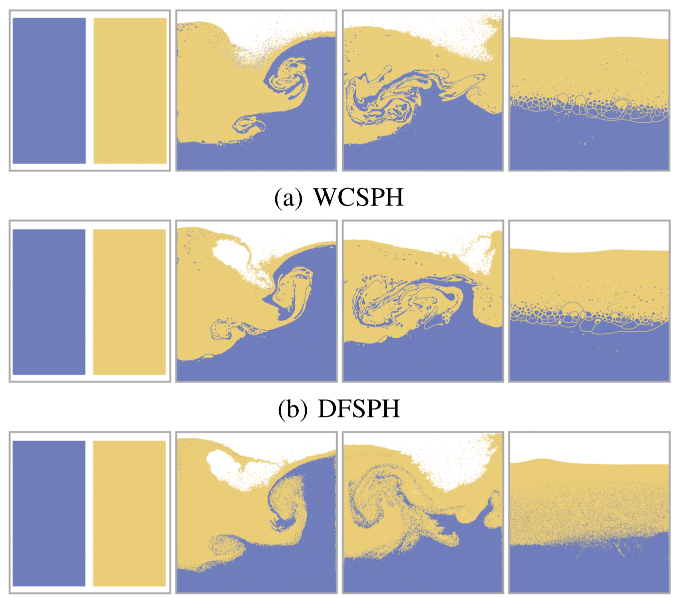

(a) WCSPH

(b) DFSPH

(c) Volume-incompressible SPH

Fig. 4. Two-phase coupling experiment.

A. Two-phase Coupling Experiment

The experiment in Figure 4 verifies the superiority of the volume-incompressible SPH method to the traditional WCSPH and DFSPH methods. The two fluid phases are respectively colored yellow and blue with a density ratio of $1 : 2$. Diffusion and surface tension are disabled. In the experiment, two blocks of fluid, each consisting of one phase, fall freely into the container to interact with each other.

From Figure 4, it can be seen that in WCSPH, the yellow phase's surface is unstable. Moreover, due to the poor pressure handling at the phase interface, WCSPH and DFSPH generate unnatural thin artifacts, and cause an excess of bubbles where surface tension should not be present. Our volume-incompressible method avoids these problems and shows smoother coupling details, indicating a more stable pressure calculation between phases.

Figure 5 shows the statistics about efficiency and conservation of energy of different methods. Firstly, Figure 5 shows the time consumption of running one frame of simulation. It can be seen that the efficiency of our method is similar to DFSPH, and about two times better than WCSPH. Secondly, Figure 5 pictures the evolution of the ratio of total mechanical energy of all particles, showing the percentage of mechanical energy remaining compared to frame 30. The total mechanical energy decreases over time due to viscosity and numerical dissipation. Our method retains the most mechanical energy, meaning our method has less numerical dissipation, and thus a better numerical accuracy.

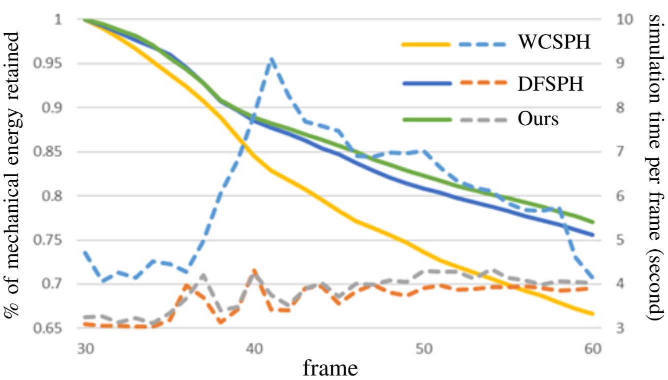

Fig. 5. Comparison of the time consumption per frame of simulation and mechanical energy between WCSPH, DFSPH and our volume-incompressible SPH.

This experiment shows that our method can efficiently simulate the two-phase coupling between silicone oil and water, and has better simulation accuracy than the WCSPH and DFSPH methods.

B. Ink Drop Experiment

The experiment in Figure 6 simulates the diffusion process of a red ink droplet falling into water and demonstrates the diffusion effect in our method.

Ink and water are respectively colored red and white, with a density ratio of $2:1$. The top row has no diffusion, while the middle and bottom row set the diffusion coefficient D_m at 0.003 and 0.005 respectively to control the diffusion rate. As can be seen in Figure 6, the larger D_m is, the more rapid the diffusion process is.

This experiment shows that our multiphase mixture model can effectively simulate diffusion effects, with a controllable diffusion rate.

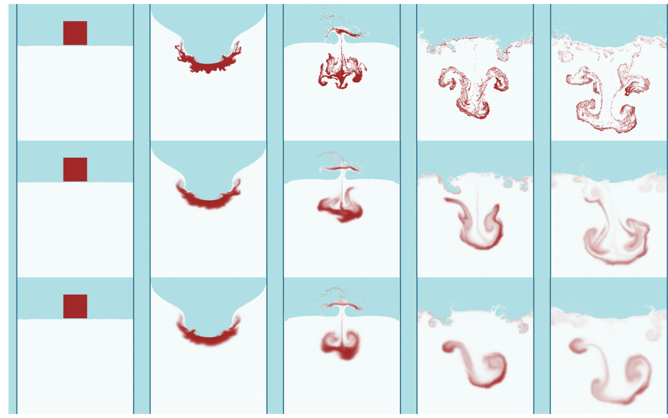

Fig. 6. Ink drop experiment. Top row: no diffusion. Middle row: diffusion parameter $D_m = 0.003$. Bottom row: $D_m = 0.005$

C. Silicone Oil Tamponade and Emulsification Experiment

This experiment simulates the silicone oil tamponade operation and the postoperative silicone oil emulsification. The experiment is performed on an eye model shown in Figure 7 (a); and the content of the eye during the simulation is displayed in cross section. Density of water and silicone oil are respectively set at 1.000 g/mL and 0.963 g/mL. The surface tension coefficient γ and diffusion parameter D_m are intuitively set at $\gamma = 3$ and $D_m = 0.01$ to model the strong surface tension and slow emulsification of silicone oil.

We first simulate the silicone oil tamponade in Figure 7 (b), (c). In the simulation, silicone oil (white) is injected into the vitreous cavity filled with water (blue) after vitrectomy. The silicone oil and water are set to be non-diffusible during this process since the surgery's duration is too short for any visible emulsification to happen. Here we also demonstrate the surface tension effect. In Figure 7 (b), there is no surface tension, i.e. surface tension coefficient $\gamma = 0$, while in Figure 7 (c), surface tension is enabled for silicone oil, which exhibits a realistic bubble-like shape, correctly modeling the surface

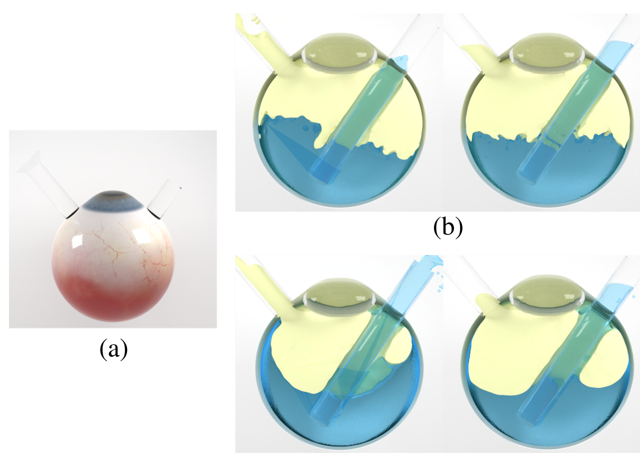

(a)

(b)

(c)

Fig. 7. Silicone oil tamponade experiment. (a): eye model used; (b) no surface tension; (c) surface tension coefficient $\gamma = 3$.

tension effect.

Next, we turn the eye model to correspond to the prone position after surgery, and enable diffusion for the surface tension scene. The result is shown in Figure 8. In this experiment, we can see that the silicone oil is slowly emulsified; and the emulsified silicone oil gradually diffuses into the water. With this simulation, we can estimate the state of silicone oil emulsification within the eye.

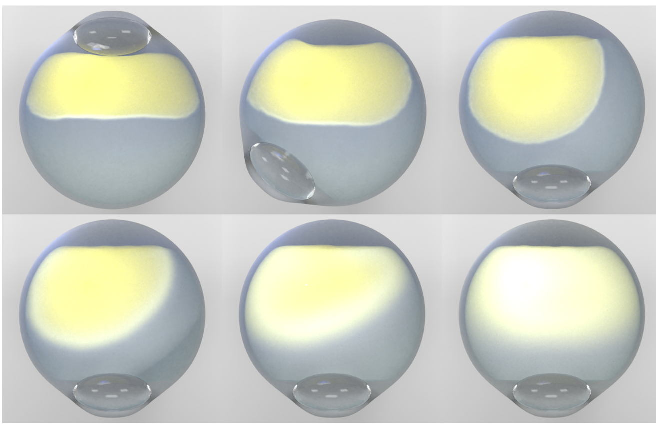

Fig. 8. Silicone oil emulsification experiment.

V. Conclusion

To help people better understand the process of silicone oil tamponade and silicone oil emulsification, we present a simulation and visualization method for the interaction and emulsification between silicone oil and water during and after silicone oil tamponade. We propose a volume-incompressible multiphase fluid simulation framework to simulate silicone oil-water coupling, use cohesion and curvature force to achieve surface tension effects, and introduce a volume fraction-based mixture model to realize the simulation of silicone oil emulsification in the intraocular cavity. Experiment results show that our method can effectively and stably realize the simulation and visualization of silicone oil-water coupling, surface tension, emulsification and diffusion.

Our simulation method can be used to demonstrate silicone oil tamponade and its complications, and to predict the emulsification state of silicone oil in the intraocular cavity after surgery. Further research can consider the varying physical properties of different types of silicone oil, and the patient's intraocular condition, to determine the simulation parameters for individual cases.

Acknowledgment

This research was supported by: Key Research Plan of Hainan Province (ZDYF2020031, ZDYF2019009), National Science Foundation of China (61873299), Science Foundation of Guangdong (2021A1515012285), Scientific and Technological Innovation Foundation of Shunde Graduate School, USTB (BK20AF001, BK19AE034), Fundamental Research Funds for the Central Universities of China (FRF-TP-19-043-A2), Development Program of China (2019YFC0605301).

References

[1] R. Machemer, H. Buettner, E. Norton, and J.-M. Parel, "Vitrectomy: a pars plana approach," Transactions - American Academy of Ophthalmology and Otolaryngology. American Academy of Ophthalmology and Otolaryngology, vol. 75, pp. 813–20, 07 1971.

[2] P. CIBIS, B. BECKER, E. OKUN, and S. CANAAN, "The use of liquid silicone in retinal detachment surgery," Archives of ophthalmology, vol. 68, pp. 590–9, 12 1962.

[3] J. B. Miller, T. D. Papakostas, and D. G. Vavvas, "Complications of emulsified silicone oil after retinal detachment repair," in Seminars in ophthalmology, vol. 29, no. 5-6. Taylor & Francis, 2014, pp. 312–318.

[4] P. Jr, D. Hatchell, G. Foulks, and M. III, "The effect of silicone oil on the cornea," Archives of Ophthalmology, vol. 103, pp. 90–94, 04 1985.

[5] C.-S. Yang, K.-H. Chen, W.-M. Hsu, and Y.-S. Li, "Cytotoxicity of silicone oil on cultivated human corneal endothelium," Eye (London, England), vol. 22, pp. 282–8, 03 2008.

[6] M. Kawaguchi, "Silicone oil emulsions stabilized by polymers and solid particles," Advances in Colloid and Interface Science, vol. 233, 07 2015.

[7] D. Odrobina, J. Golebiewska, and I. Maroszynska, "Choroidal thickness changes after vitrectomy with silicone oil tamponade for proliferative vitreoretinopathy retinal detachment," Retina, vol. 37, p. 1, 12 2016.

[8] J. Monaghan, "Smoothed particle hydrodynamics," Reports on Progress in Physics, vol. 68, p. 1703, 07 2005.

[9] M. Becker and M. Teschner, "Weakly compressible sph for free surface flows," in Proceedings of the 2007 ACM SIGGRAPH/Eurographics Symposium on Computer Animation, vol. 9, 01 2007, pp. 209–217.

[10] B. Solenthaler and R. Pajarola, "Predictive-corrective incompressible sph," ACM Trans. Graph., vol. 28, 07 2009.

[11] M. Ihmsen, J. Cornelis, B. Solenthaler, C. Horvath, and M. Teschner, "Implicit incompressible sph," IEEE transactions on visualization and computer graphics, vol. 20, 07 2013.

[12] J. Bender and D. Koschier, "Divergence-free smoothed particle hydrodynamics," in ACM SIGGRAPH/Eurographics Symposium on Computer Animation, 08 2015.

[13] M. Müller, B. Solenthaler, R. Keiser, and M. Gross, "Particle-based fluid-fluid interaction," in Proceedings of the 2005 ACM SIGGRAPH/Eurographics Symposium on Computer Animation, 01 2005, pp. 237–244.

[14] S. Liu, Q. Liu, and Q. Peng, "Realistic simulation of mixing fluids," The Visual Computer, vol. 27, pp. 241–248, 03 2011.

[15] B. Ren, C.-F. Li, X. Yan, M. Lin, J. Bonet, and S.-M. Hu, "Multiple-fluid sph simulation using a mixture model," ACM Transactions on Graphics, vol. 33, pp. 1–11, 09 2014.

[16] Y. Jiang, C. Li, S. Deng, and S. Hu, "A divergence-free mixture model for multiphase fluids," Computer Graphics Forum, vol. 39, pp. 69–77, 12 2020.

[17] T. Yang, J. Chang, B. Ren, M. Lin, J. Zhang, and S.-M. Hu, "Fast multiple-fluid simulation using helmholtz free energy," ACM Transactions on Graphics, vol. 34, pp. 1–11, 10 2015.

[18] W. Li, D. Liu, M. Desbrun, J. Huang, and X. Liu, "Kinetic-based multiphase flow simulation," IEEE Transactions on Visualization and Computer Graphics, vol. PP, pp. 1–1, 02 2020.

[19] D. Koschier, J. Bender, B. Solenthaler, and M. Teschner, "Smoothed particle hydrodynamics techniques for the physics based simulation of fluids and solids," in Eurographics - Tutorials, 05 2019.

[20] S. Band, C. Gissler, M. Ihmsen, J. Cornelis, A. Peer, and M. Teschner, "Pressure boundaries for implicit incompressible sph," ACM Transactions on Graphics, vol. 37, pp. 1–11, 02 2018.

[21] N. Akinci, G. Akinci, and M. Teschner, "Versatile surface tension and adhesion for sph fluids," ACM Transactions on Graphics, 10 2013.

[22] M. Mikko, V. Taivassalo, and S. Kallio, "On the mixture model for multiphase flow," VTT Publications, vol. 288, 01 1996.

[23] Y. Hu, T.-M. Li, L. Anderson, J. Ragan-Kelley, and F. Durand, "Taichi: a language for high-performance computation on spatially sparse data structures," ACM Transactions on Graphics, vol. 38, pp. 1–16, 11 2019.

[24] X. Wang, X. Ban, X. Liu, Z. Yalan, and L. Wang, "Effective reconstructing surfaces algorithm of anisotropic kernels orienting sph fluids," Journal of Computer-Aided Design and Computer Graphics, vol. 28, pp. 1497–1505, 09 2016.